# Pathways Involved in Targeting and Secretion of a Lysosomal Enzyme in *Dictyostelium Discoideum*

ROBERT C. MIERENDORF, JR., JAMES A. CARDELLI, and RANDALL L. DIMOND
*Department of Bacteriology, University of Wisconsin, Madison, Wisconsin 53706. Dr. Mierendorf's present address is Promega Biotec, Madison, Wisconsin 53711.*

ABSTRACT In *Dictyostelium discoideum*, the lysosomal enzyme α-mannosidase is first synthesized as an N-glycosylated precursor of $M_r$ 140,000. After a 20–30-min lag period, up to 30% of the precursor molecules are rapidly secreted, whereas the rest remain cellular and are proteolytically processed ($t_{1/2}$ = 8 min) to mature subunits of $M_r$ 58,000 and 60,000. The secreted precursor is modified more extensively than the cellular form, as is revealed by differences in size, charge, and sensitivity to endoglycosidase H. Subcellular fractionation has shown that, following synthesis in the rough endoplasmic reticulum, the precursor is transported to a low density membrane fraction that contains Golgi membranes. Proteolytic processing takes place in these vesicles, since newly cleaved mature enzyme, but no precursor, co-fractionates with lysosomes. Under conditions that disrupt vesicular membranes, the precursor remains associated with the membrane fraction, whereas the newly processed mature enzyme is soluble. Proteolytic cleavage of the precursor thus coincides with the release of the mature enzyme into the lumen of a lysosomal compartment. These findings suggest a possible mechanism for lysosomal targeting that involves the specific association of enzyme precursors with Golgi membranes.

Many lysosomal enzymes are synthesized as precursor molecules, which are subsequently modified and proteolytically processed intracellularly to their mature forms (9, 24, 30, 38, 43). However, some uncleaved precursor molecules often accumulate extracellularly (24). Many cell types contain specific membrane receptors that recognize mannose-6-phosphate residues on the N-linked oligosaccharide side chains of lysosomal enzymes (12, 14, 27, 37). Several lines of evidence have pointed to the involvement of these receptors in the capture of newly synthesized enzymes and subsequent targeting to their intracellular destination as mature forms in lysosomes (13, 35, 42). However, this is probably not the only functional targeting mechanism, since there are examples of cells lacking receptors that still localize the enzymes normally (19). The subcellular sites where the modification and cleavage events occur, how these events are coordinated, and what role they have in targeting and secretion of these enzymes remain to be fully elucidated.

The cellular slime mold, *Dictyostelium discoideum*, is a simple eucaryote that possesses a well developed lysosomal system (7). In this organism the lysosomal enzyme α-mannosidase is synthesized as a $M_r$ 140,000 precursor that is proteolytically cleaved to mature subunits of $M_r$ 60,000 and 58,000 (30, 32). The precursor is synthesized on membrane bound polysomes and consists of a $M_r$ 120,000 polypeptide backbone to which ~20,000 mol wt of N-linked high mannose oligosaccharide side chains have been added cotranslationally (Cardelli, J. A., R. C. Mierendorf, Jr., and R. L. Dimond, manuscript submitted for publication). In axenic (broth) cultures as much as 70% of the total α-mannosidase activity is extracellular (5). Whereas both precursor and mature enzyme forms are found in the medium, almost no precursor accumulates in the cells. The precursor is enzymatically active and accounts for up to 20% of the total extracellular activity (30). The mature enzyme contains mannose-6-phosphate and binds with high affinity to mammalian phosphomannosyl receptors (16). However, a number of laboratories have failed to find any evidence for a similar phosphomannosyl receptor in *D. discoideum*. Thus, the organism appears to resemble some mammalian cell lines that target lysosomal enzymes by an alternate mechanism.

In this report we describe some of the events that follow enzyme synthesis and affect the processing and secretion of the α-mannosidase precursor. We studied the kinetics of precursor secretion and proteolytic cleavage, the modification of secreted precursor relative to the cellular form, and the

subcellular location of the divergence of the secretory and proteolytic processing pathways. We propose a mechanism whereby lysosomal enzymes are localized in *Dictyostelium* without the involvement of phosphomannosyl receptors.

## MATERIALS AND METHODS

*Organism:* Strains of *D. discoideum* were grown axenically in TM medium (15) at 21°C on a rotary shaker at 200 rpm. In addition to the wild-type parental strain, Ax3, the α-mannosidase structural gene mutant M4 (15) was used as indicated.

*Radioactive Labeling:* For pulse-labeling of proteins, logarithmically growing cells were collected by centrifugation (1,000 *g*, 3 min) and resuspended at 5–10 × $10^6$ cells/ml in fresh TM medium containing 500–800 μCi/ml of [$^{35}$S]methionine (Amersham Corp., Arlington Heights, IL; 1,200 Ci/mmol). After incubation at 21°C for the times indicated in the figure legends, the cells were quickly collected by centrifugation and either processed immediately or, when a chase period was required, resuspended at 5 × $10^6$ cells/ml in fresh medium without the isotope followed by continued incubation. Under these conditions, there was a maximum of 15% (usually 0–5%) additional incorporation during the chase as measured by total trichloroacetic acid precipitable counts per minute. Samples containing equal numbers of counts per minute were used for immunoprecipitation in these experiments.

Quantitative measurements of band intensities were performed using a computer interfaced LKB Model 2202 Ultroscan laser densitometer (LKB Instruments, Inc., Gaithersburg, MD with the aid of the Vidichart peak integration program (Interactive Microware, Inc., State College, PA). Bands were scanned across their widths to provide accurate readings.

*Immunoprecipitation and Electrophoresis:* α-Mannosidase was immunoprecipitated from crude cellular and secreted protein samples using polypeptide specific monoclonal antibodies (30, 31) and Pansorbin (Calbiochem-Behring Corp., San Diego, CA). All procedures were carried out at 0–4°C. Samples were treated with 1% Triton X-100 and incubated briefly with 0.1 vol of Pansorbin, followed by centrifugation at 10,000 *g* for 3 min. The supernatants were removed to fresh tubes and excess monoclonal antibodies ($IgG_{2a}$ or $IgG_{2b}$ subclasses) added. After 30–60 min, 50 μl Pansorbin was added and incubation continued for another 30–60 min. The Pansorbin was collected by centrifugation and washed three times with a solution containing 10 mM Tris-HCl, pH 8.0, 150 mM NaCl, 0.5% Nonidet P-40 (0.75 ml). The final pellet was resuspended in gel sample buffer (250 mM Tris-HCl, pH 6.8, 4% SDS, 10% β-mercaptoethanol, and 30% sucrose) and heated to 80°C for 3 min. After centrifugation, the eluted samples were subjected to SDS PAGE (7.5% acrylamide) according to Laemmli (28). Gels were fixed in 10% trichloroacetic acid, treated with Enhance (New England Nuclear; Boston, MA), dried under vacuum and exposed to Kodak XAR-5 x-ray film at −70°C.

*Cell Fractionation:* Growing cells were harvested by centrifugation (1,000 *g*, 3 min), washed once in a solution containing 50 mM Tris-HCl, pH 7.5, 25 mM KCl, 5 mM $MgCl_2$ (TKM)[1] plus 0.25 M sucrose, and resuspended at a concentration of 2–4 × $10^8$ cells/ml in the same buffer (all procedures at 0–4°C). When fractionating radioactively labeled wild-type cells (usually a total of 1–5 × $10^7$ cells), a 10–100-fold excess of unlabeled cells of the α-mannosidase structural gene mutant, M4, were added to facilitate handling. The mutant cells do not accumulate α-mannosidase protein. The cells were broken using a tight fitting Dounce homogenizer (15 strokes) and nuclei and unbroken cells were removed by centrifugation (1,000 *g*, 5 min). Two cycles of homogenization consistently resulted in breakage of 70–80% of the cells. The postnuclear supernatant was layered on top of 7 ml TKM plus 0.5 M sucrose in a tube that also contained a 0.25-ml cushion of TKM plus 2.5 M sucrose and centrifuged in a Beckman SW 40 rotor (Beckman Instruments, Inc., Palo Alto, CA) at 100,000 *g* for 30 min. The supernatant was removed and the collected membranes at the cushion interface were resuspended in 1.8 ml TKM. The membrane sample was applied to a discontinuous sucrose gradient consisting of 2.0 ml each of TKM containing 1.8, 1.5, 1.3, 1.1, and 0.8 M sucrose, respectively. After centrifugation at 100,000 *g* for 2.5 h, the gradients were fractionated from the top, the fractions were diluted with equal volumes of TKM and centrifuged again at 100,000 *g* for 30 min in a Beckman Ti 50 rotor to concentrate the membranes. The supernatants were removed and pellets resuspended in 10 mM Tris-HCl, pH 8.0, 150 mM NaCl, 1% Triton X-100, and used for immunoprecipitation. In some cases the fractions were assayed directly for marker enzymes. α-Mannosidase was assayed as described by Loomis (29), α-glucosidase-2 as described by Borts and Dimond (2), and NADH cytochrome *c* reductase as described by Amar-Costesec et al. (1).

[1] *Abbreviations used in this paper:* endo H, endoglycosidase H; RER and SER, rough and smooth endoplasmic reticulum, respectively; TKM, 50 mM Tris-HCl, pH 7.5, 25 mM KCl, 5 mM $MgCl_2$.

## RESULTS

### Secretion vs. Processing of the α-Mannosidase Precursor

The fate of newly synthesized α-mannosidase in axenically growing cells was studied by a pulse-chase protocol in which cultures in late log phase were labeled for short periods of time with [$^{35}$S]methionine (pulse) followed by incubation in the absence of isotope for various intervals (chase). Fig. 1 shows the results of two experiments with different pulse and chase periods. Fig. 1 *A* shows a short term experiment in which cells were labeled for 10 min and chased over the next 45 min, while in Fig. 1 *B* the pulse was for 20 min and the chase covered the following 6 h. At each time point the cells and media were separated by centrifugation and samples immunoprecipitated with a monoclonal antibody specific for α-mannosidase followed by SDS PAGE and fluorography. The relative intensities of the immunoprecipitated α-mannosidase bands as seen on x-ray film exposed to the gel were quantitated by laser densitometry (Fig. 1, *C* and *D*). It is clear that the conversion of the $M_r$ 140,000 precursor to the mature $M_r$ 60,000 and 58,000 subunits occurred intracellularly following an initial lag period of ~20–30 min. From these and other experiments (not shown) the data indicate that following the initial lag the cellular precursor was processed with a half life of ~8 min with a concomitant accumulation of the mature $M_r$ 58,000 and 60,000 proteins. However, while 70–80% of the total precursor remained cellular and underwent proteolytic processing, a portion escaped processing and was rapidly secreted, first appearing in the medium within 10 min, as seen in lane 7 of Fig. 1 *A*. Fig. 1, *C* and *D*, show that the secreted precursor accumulated quickly during the next 20 min and then either remained at this level or rose very slowly over the next few hours. In contrast, the mature enzyme began to appear in the medium after ~2 h and then accumulated only gradually. This dramatic difference in the kinetics of secretion indicates that the extracellular forms of the enzyme are derived from separate secretory pools.

The presence of a 20–30-min delay between the synthesis of the $M_r$ 140,000 precursor and the beginning of its conversion to the mature subunits indicates that these two processes probably occur at different sites. This delay was also observed when the accumulation of label in the precursor and mature forms of α-mannosidase was observed under conditions in which [$^{35}$S]methionine was present continuously (data not shown).

Besides being secreted by cells growing in nutrient containing medium, lysosomal enzymes are also very efficiently secreted when growing cells are placed in a starvation buffer (7). These conditions stimulate the secretion of 60% +/− 14% of the total α-mannosidase activity within 4 h in the absence of additional enzyme synthesis (Ebert D. L., and R. L. Dimond, unpublished data). To follow the processing and secretion of newly synthesized enzyme under starvation conditions, we pulse-labeled cells for 20 min as above, but the chase was carried out in phosphate buffer lacking nutrients. Fig. 2 *A* shows that the kinetics of processing and secretion of the precursor and mature forms are comparable to those found under growth conditions. While the precursor was rapidly secreted, the mature enzyme only began to appear after 2 h.

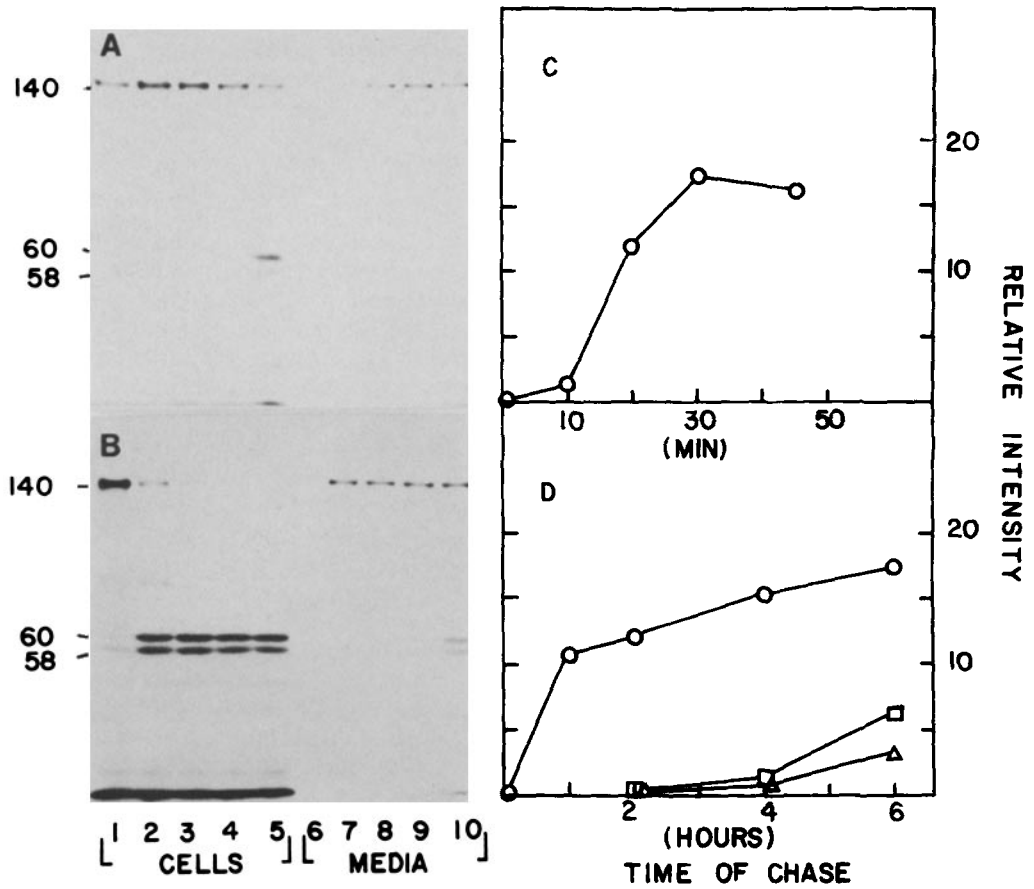


FIGURE 1 Processing and secretion of the α-mannosidase precursor. Axenically growing cells were pulse-labeled with [$^{35}$S]-methionine and then incubated in unlabeled medium as described in Materials and Methods. At various intervals, samples were removed and the cells separated from the medium by centrifugation. α-Mannosidase was immunoprecipitated from all samples and subjected to electrophoresis on 7.5% SDS polyacrylamide gels followed by fluorography to visualize the labeled enzyme forms. (*A*) Cells pulse-labeled for 10 min, and chased for 0, 10, 20, 30, and 45 min. (*B*) Cells pulse-labeled for 20 min, and chased for 0, 1.0, 2.0, 4.0, and 6.0 h. In *A* and *B*, lanes *1–5* are cellular samples at the indicated time points, and lanes *6–10* are samples of the medium from the same time points in the same order. *C* and *D* quantitate the amount of secreted polypeptides (lanes *6–10* in *A* and *B*, respectively), as determined by laser densitometry. O, 140-kD precursor; □, 60-kD subunit; △, 58-kD subunit.

These results are in agreement with those of Wood et al. (45), who found a 3–4-h lag between synthesis and secretion of the bulk of mature α-mannosidase. Additional experiments in which the chase under starvation conditions was delayed for various amounts of time after the pulse demonstrated that >90% of the labeled $M_r$ 58,000 and 60,000 subunits were eventually secreted (results not shown).

Fig. 2*B* shows the results of a similar analysis done in the presence of three known inhibitors of secretion. Pulse-labeled cells were chased for 30 min in phosphate buffer containing 25 mg/ml trypticase in lanes *1* and *2*, 5 mM sodium azide in lanes *3* and *4*, or 5 mM potassium cyanide in lanes *5* and *6* in Fig. 2*B*. Each of these conditions drastically reduces the secretion of several lysosomal enzymes, including α-mannosidase, in this system (7). The presence of exogenous nutrients in the form of trypticase only slightly affected the secretion of the precursor (compare with lanes *3* and *9* in Fig. 2*A*), but appeared to affect processing by allowing the accumulation of an α-mannosidase species of $M_r$ ~80,000. The $M_r$ 80,000 species is usually observed as a faint diffuse band that appears and disappears with kinetics consistent with a role as a processing intermediate between the precursor and $M_r$ 58,000 and 60,000 products (32; see also Fig. 2*A*). Whereas the addition of trypticase produced these relatively minor effects, the metabolic inhibitors completely prevented both the secretion and proteolytic processing of the precursor, indicating an energy requirement for both events.

## Differences between Cellular and Secreted Precursors

The results in the preceding section demonstrated that ~10–30 min after the α-mannosidase $M_r$ 140,000 precursor is synthesized, some molecules (~20%) are rapidly secreted while the rest enter the intracellular processing pathway. The different pathways followed by the precursor may either depend on or lead to differences in posttranslational modification. Fig. 3 shows two examples of such differences. In Fig. 3*A* the apparent sizes of steady-state-labeled secreted (Fig. 3*A*, lane *1*) and pulse-labeled cellular (Fig. 3*A*, lane *2*) α-mannosidase were directly compared by SDS PAGE. While the $M_r$ 58,000 and 60,000 forms were identical in migration, the cellular precursor migrated slightly faster than its secreted counterpart. It is difficult to quantitate the apparent size difference in this region of the gel, but the cellular form appears to be between 2,000 and 5,000 daltons smaller than the secreted precursor. In pulse-chase experiments, the newly secreted precursor was identical in size to the steady-state-

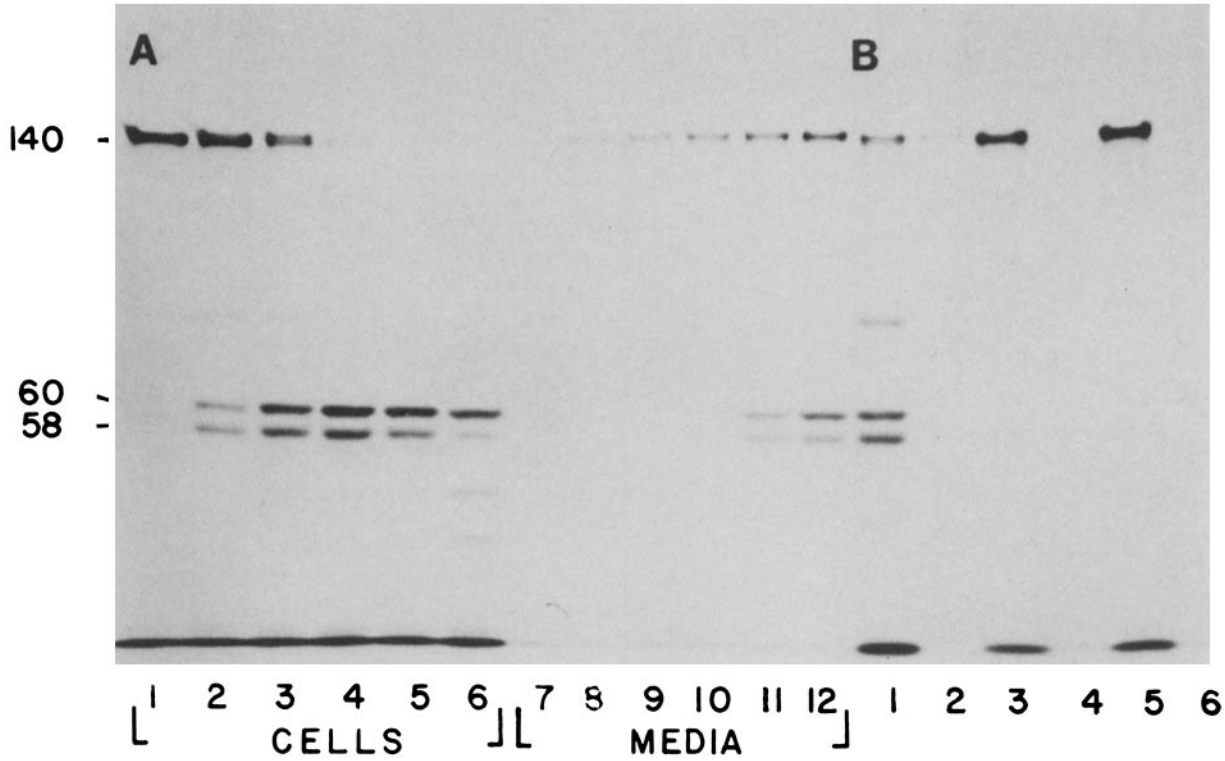


FIGURE 2 Processing and secretion of pulse-labeled α-mannosidase under starvation conditions. Axenically growing cells were pulse-labeled for 20 min with [$^{35}$S]met, collected by centrifugation, washed once in 10 mM potassium phosphate (pH 6.5), and resuspended at a final concentration of $10^7$ cells/ml in this same buffer. Incubation was continued at 24°C and samples were removed at 0, 15, 30, 60, 120, and 240 min. The cells were separated from the medium by centrifugation and α-mannosidase was immunoprecipitated from each sample followed by SDS PAGE and fluorography. (*A*) Lanes *1–6* are cellular samples and lanes *7–12* are secreted (medium) samples taken at the indicated time points in the same order. (*B*) After the 20-min labeling period, the cells were chased for 30 min in starvation buffer containing (lanes *1* and *2*) 25 mg/ml trypticase, (lanes 3 and *4*) 5 mM sodium azide, or (lanes *5* and 6) 5 mM potassium cyanide. The first lane of each pair is the cellular sample and the second is the secreted (medium) sample.

labeled secreted precursor in Fig. 3 (data not shown). In Fig. 3*B* the various enzyme forms were immunopurified and exhaustively digested with endoglycosidase H (endo H), an enzyme that cleaves N-linked mannose-rich oligosaccharide side chains. When incubated with endo H, most pulse-labeled cellular precursor shifted to an apparent $M_r$ of ~120,000 (Fig. 3*B*, lane *3*), which is similar to the unglycosylated α-mannosidase polypeptide synthesized by translation in vitro, shown in Fig. 3*B*, lane *1*. In contrast, lane *5* shows that the secreted $M_r$ 140,000 precursor shifted only slightly when treated with endo H. In addition, the $M_r$ 58,000 subunit was much more sensitive than the $M_r$ 60,000 species in both cellular and secreted samples.

The above data indicate that the ~20,000 daltons of carbohydrate added cotranslationally to the cellular precursor polypeptide is completely removed by endo H treatment, while the oligosaccharides are much more resistant on the secreted precursor. The mechanism of endo H resistance in *Dictyostelium* enzymes appears to be the presence of esterified sulfate on the N-linked mannose-rich oligosaccharide side chains rather than further carbohydrate modifications producing more complex structures (17). These molecules also contain variable amounts of esterified phosphate (17), which, in combination with the sulfate, contributes to the highly acidic character of the enzymes. Accordingly, differences in charge between the cellular and secreted precursors would suggest differences in their degree of sulfation and/or phosphorylation. The analysis of immunopurified cellular and secreted precursors by two-dimensional gel electrophoresis displayed in Fig. 4 shows that the cellular form in Fig. 4*A* had a higher isoelectric point than the secreted form in Fig. 4*B*, which indicates that it is indeed less negatively charged.

## *Intracellular Transport Pathway for the α-Mannosidase Precursor*

A more detailed study of the intracellular route taken by newly synthesized precursor molecules was required to determine which subcellular compartments are involved in the posttranslational events leading to modification, processing, and secretion. α-Mannosidase is synthesized on membrane bound polysomes and is cotranslationally glycosylated (Cardelli, Mierendorf, and Dimond, manuscript submitted for publication). In preliminary studies, we found that >95% of the pulse-labeled cellular precursor cofractionated with crude postnuclear membrane vesicles collected by centrifugation at 100,000 *g*. These vesicles can be fractionated by centrifugation on discontinuous sucrose gradients (Cardelli, Mierendorf, and Dimond, manuscript in preparation).

Fig. 5 shows such a fractionation performed with cells that had been pulse-labeled with [$^{35}$S]methionine for 10 min. Fig. 5, *A* and *B*, display the distribution of the α-mannosidase precursor and several marker enzymes, respectively, under normal fractionation conditions. The two marker enzymes

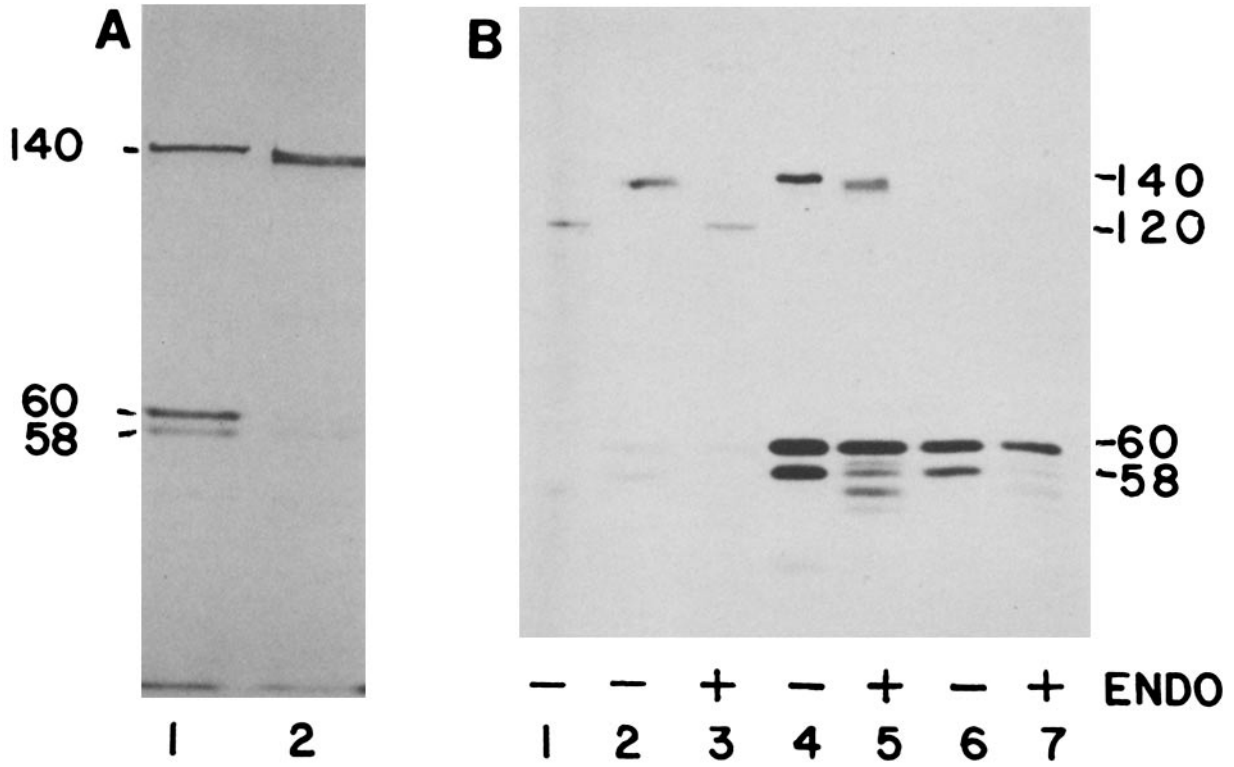


FIGURE 3 Differences in modification between cellular and secreted precursors. (*A*) Difference in size. α-Mannosidase was immunoprecipitated from spent medium from cells grown axenically in the presence of [$^{35}$S]met for five generations (lane *1*) and axenically growing cells pulse-labeled for 30 min (lane *2*). (*B*) Difference in sensitivity to endo H. Lane *1*, the α-mannosidase primary translation product (120 kD) immunoprecipitated from products synthesized in vitro in the presence of [$^{35}$S]met by a rabbit reticulocyte lysate primed with total RNA extracted from axenically growing cells; lanes *2* and *3*, α-mannosidase immunoprecipitated from cells pulse-labeled for 20 min; lanes *4* and *5*, α-mannosidase from the spent medium of a culture labeled for 48 h; lanes 6 and *7*, α-mannosidase from growing cells labeled for 48 h. The samples in lanes *4–7* were immunopurified by affinity chromatography on a column of monoclonal antibody coupled to agarose. Where indicated (lanes *3*, *5*, and *7*), the immunopurified samples were suspended in 0.2 M citrate (pH 5) and incubated with 2.5 mU of endo H overnight at 37°C. All samples were subjected to electrophoresis on a 7.5% SDS polyacrylamide gel followed by fluorography.

for microsomes, α-glucosidase-2 (2, 8, 22) and NADH cytochrome *c* reductase (1), both appeared near the bottom of the gradient, consistent with the high density of rough endoplasmic reticulum (RER). The bulk (80%) of the pulse-labeled precursor was also found in the bottom fractions, consistent with its synthesis on membrane bound polysomes. Further evidence for this view is presented in Fig. 5, *C* and *D*. Before centrifugation of these samples, the resuspended 100,000 *g* pellet fractions were treated with 10 mM EDTA, a procedure that dissociates ribosomes from their membrane-binding sites (41). Fig. 5 *D* shows that the ER marker enzymes shifted to the low density membrane fraction following EDTA treatment consistent with the removal of dense ribosomes, while the lysosomal marker (α-mannosidase) remained near the middle of the gradient. Similarly, the α-mannosidase precursor shifted to the low density fraction as shown in Fig. 5 *C*, strongly suggesting that it is associated with the same class of vesicles as the ER markers.

As seen in Fig. 5 *A*, a portion of the pulse-labeled precursor is normally found in the light membrane fraction, which may represent material that has been transferred from the RER to this compartment during the 10-min labeling period. To explore whether the precursor in fact follows this pathway, we carried out fractionations after chase periods of 20 and 40 min subsequent to a 10-min pulse. Fig. 6 *A* shows the distribution of the precursor at the end of the labeling period. The marker enzymes assayed in each experiment in this figure had the same distribution as that shown in Fig. 5 *B*. As in Fig. 5, most molecules appeared first in the RER fractions where they were synthesized. After a 20-min chase (Fig. 6 *B*), most of the precursor had shifted to the low density membrane fraction. The transfer to this compartment precedes the appearance of the mature enzyme, which had begun by 40 min (Fig. 6 *C*). The distribution of the newly processed mature enzyme closely paralleled that of the bulk enzyme activity as seen in Fig. 5, which suggests that proteolytic processing coincides with transport to lysosomes.

These data suggest that the site of divergence of the secretory and processing pathways may reside within the low density membrane compartment. Further evidence for this conclusion is presented in Fig. 7. In this experiment, cells were pulse-labeled for 10 min followed by a chase period of 1 h in the presence of 5 mM potassium cyanide, a condition that blocks the conversion of the precursor to mature enzyme as well as its secretion as seen in Fig. 2 *B*. As in the preceding experiments, the cells were fractionated and the distribution of the precursor across the gradient determined. The results show that the inhibitor caused the accumulation of the precursor in the low density membrane fractions, indicating a block subsequent to transport from the RER but before lysosomal localization. It seems likely that transport from RER to the low density membrane compartment is not an energy-requir-

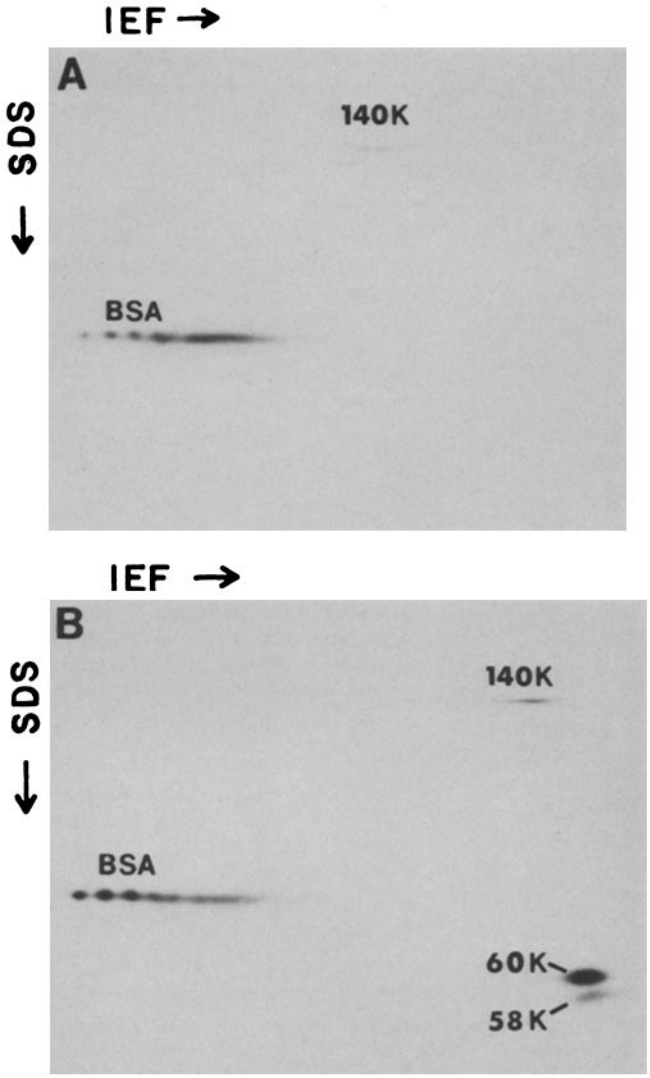


FIGURE 4 Difference in isoelectric point between cellular and secreted precursors. α-Mannosidase was immunopurified by affinity chromatography on antibody-agarose and subjected to two-dimensional electrophoresis by the method of O'Farrell (33) with minor modifications, followed by fluorography. (*A*) Cellular precursor pulse-labeled with [$^{35}$S]met for 20 min. (*B*) Secreted α-mannosidase isolated from spent medium of a culture labeled for 48 h. [$^{14}$C]-labeled BSA (New England Nuclear) was added to the samples before electrophoresis as an internal marker. The acidic end of the gel is to the right.

ing process, in contrast to subsequent localization steps.

The sedimentation of the low density membrane fraction between 0.8 and 1.1 M sucrose is consistent with that of Golgi membranes in other systems (6, 39). Although the Golgi marker enzyme, galactosyltransferase, is difficult to detect in growing *D. discoideum* amebae, the enzyme does accumulate in developing cells and sediments at this density (25). Another activity that appears specific for Golgi is the addition of sulfate to oligosaccharide side chains (11, 21). Two experiments designed to determine the membrane fraction in which newly synthesized α-mannosidase precursor becomes sulfated are shown in Fig. 8. For Fig. 8*A*, the precursor in different membrane fractions was tested for endo H resistance. As described above, the oligosaccharides on slime mold lysosomal enzymes acquire resistance to endo H upon sulfation (17). Cells were labeled with [$^{35}$S]methionine for 15 min followed by a 10-min chase period and fractionation by sucrose gradient sedimentation. The gradients were divided into low, medium, and high density fractions that correspond to the two top, two middle, and two bottom fractions, respectively, of Figs. 5–7. The α-mannosidase in each fraction was immunoprecipitated and incubated in the presence and absence of endo H. In the low density fraction, treatment with endo H produced a precursor form that migrated only slightly faster than the untreated form, as also observed in steady-state–labeled cells (Fig. 3). In contrast, the precursor that still remained in the high density fraction was completely converted to the unglycosylated form by endo H. In Fig. 8*B* cells were labeled for 20 min with [$^{35}$S]sulfate before fractionation to determine directly the fraction in which sulfate was added. It is clear that the low density fraction contained the bulk of sulfated precursor molecules. The data indicate that sulfate addition and the acquisition of endo H resistance occur in the low density membrane fraction. Since sulfotransferases have been localized to Golgi membranes in other systems (11, 21), we conclude that the low density membrane fraction described here consists at least in part of Golgi membranes.

As mentioned previously, the membrane fractionation experiments as performed were made possible by the near quantitative recovery of the pulse-labeled precursor in the 100,000 *g* postnuclear pellet, which was the starting material for the gradients. This raised the question whether the precursor was in fact membrane bound rather than free within vesicles, since only 70–80% of the lysosomal enzyme markers remained particulate. To address this point, we lysed pulse-labeled cells under hypotonic conditions to cause rupture of vesicular membranes, and immunoprecipitated the forms of α-mannosidase from the postnuclear 100,000 *g* pellet and supernatant fractions. Lanes 1–4 of Fig. 9 show the results of this experiment using cells labeled for 10 min, while the samples in lanes 5–8 came from cells labeled for 60 min to allow the accumulation of some newly cleaved mature enzyme. In each case the first two lanes, i.e., lanes *1* and *2* and *5* and *6*, show the pellet and supernatant fractions, respectively, from cells broken in hypotonic buffer, and the remaining lanes show the results of the lysis in isotonic buffer in the same order. Quantitation of the bands by densitometry revealed that 95% of the precursor was in the pellet fractions of 10 min samples lysed under both conditions. Similarly, almost all (99%) of the precursor was found in the membrane pellets under both lysis conditions after a 60-min labeling period. However, the hypotonic lysis released 90% of the newly processed mature enzyme into the supernatant (compare lanes *5* and *6* in Fig. 9). Under isotonic conditions, 90% of the mature form remained membrane enclosed in the pellet (compare lanes *7* and *8* in Fig. 9). In additional experiments the precursor in hypotonic membrane preparations was found to be accessible to proteolytic degradation by trypsin, indicating vesicle rupture under these conditions (data not shown).

## DISCUSSION

This report examines two alternate fates of newly synthesized α-mannosidase precursor: secretion of the intact precursor and proteolytic processing to the mature subunits that enter lysosomes. These events appear to occur with similar timing, between 20 and 30 min after the precursor is first synthesized on RER. The precursor is transported from this site to a low density membrane fraction within this same interval, and its

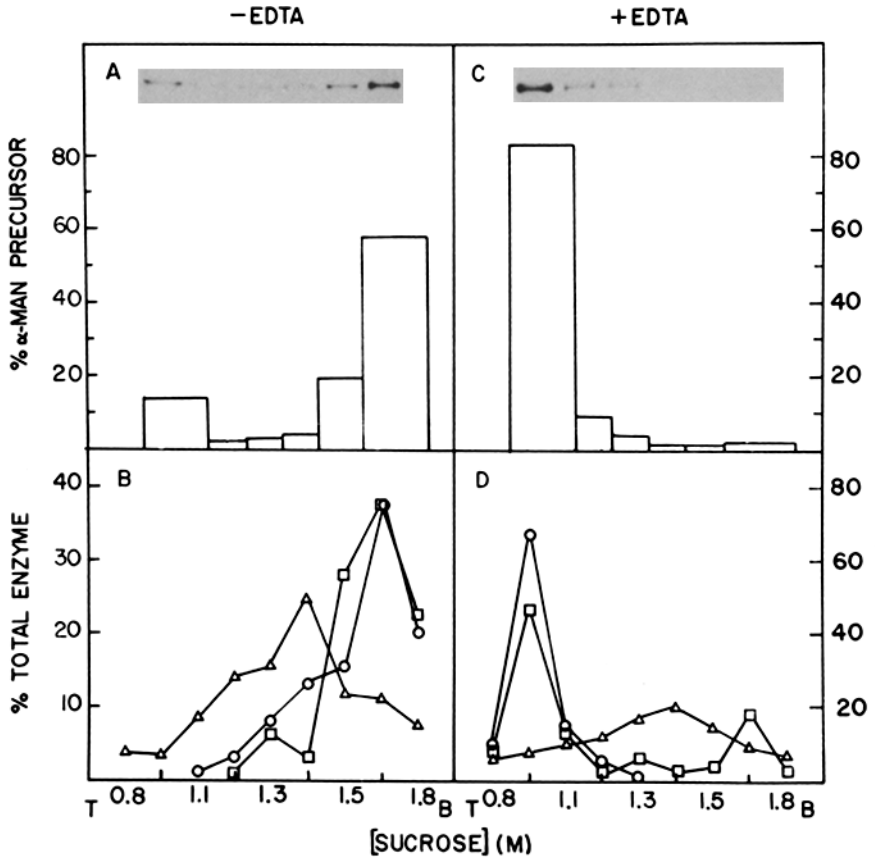


FIGURE 5 Co-fractionation of pulse-labeled α-mannosidase precursor with RER. Growing cells were pulse-labeled for 10 min with [$^{35}$S]met and then lysed using a Dounce homogenizer followed by fractionation of the postnuclear membrane vesicles collected by centrifugation at 100,000 *g* on discontinuous sucrose gradients as described in Materials and Methods. After centrifugation, the gradients were fractionated from the top in a manner corresponding to the width of the bars indicated in *A* and *C*. These two panels depict the distribution of the 140-kD α-mannosidase precursor across the gradients as detected by immunoprecipitation followed by SDS PAGE and fluorography. The percent of the total precursor present in each fraction was calculated by quantitation of the relative intensity of the precursor band in each fraction (*insets*) using laser densitometry. (*A*) Fractionation of the postnuclear membrane pellet collected after centrifugation at 100,000 *g* and resuspended in TKM buffer; (*B*) same as *A* except the membrane pellet was resuspended in the same buffer lacking $MgCl_2$ but containing 10 mM EDTA before fractionation. *C* and *D* are parallel fractionations performed with unlabeled cells and assayed for the enzymes NADH cytochrome *c* reductase (□), α-glucosidase-2 (○) and α-mannosidase (△). *T* and *B* indicate the top and bottom of the gradient, and the interfaces between different sucrose concentrations are denoted by the dividing marks.

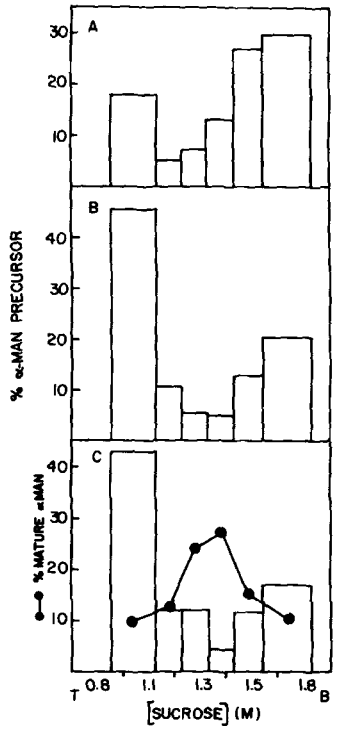


FIGURE 6 Subcellular localization of pulse-labeled α-mannosidase after chase intervals of 20 and 40 min. Axenically growing cells were pulse-labeled with [$^{35}$S]methionine for 10 min followed by continued incubation in unlabeled medium. At the end of the labeling period (*A*) and after chase periods of 20 (*B*) and 40 min (*C*), samples were removed and processed for cellular fractionation on discontinuous sucrose gradients as described in Fig. 5 and in Materials and Methods. α-Mannosidase was immunoprecipitated from each gradient fraction, subjected to electrophoresis on a 7.5% SDS polyacrylamide gel followed by fluorography, and the bands were quantitated by laser densitometry. In *C* the distribution of the newly processed mature subunits is indicated by the solid circles.

subsequent route (export vs. cleavage) appears to be determined as the precursor passes through this compartment. The major finding of these studies is that the precursor remains tightly associated with membranes until either proteolytic processing or secretion takes place.

Our results suggest that the low density compartment which is the focus of these targeting events is the Golgi complex. This organelle is contained almost exclusively within the low density fraction, based on sulfotransferase activity. This fraction may also contain smooth endoplasmic reticulum (SER) and plasma membranes, which have similar densities. Since NADH cytochrome *c* reductase, a marker for both RER and SER (22), was missing from the light fractions, it is probable that SER is not present in significant amounts in these cells. We have also followed the plasma membrane marker, alkaline phosphatase, through the fractionation and have found that most of the activity (>80%) is removed before the final sucrose gradient, although the enzyme is detectable in most of the gradient fractions (results not shown). Because this is in striking contrast to the partitioning of α-mannosidase during

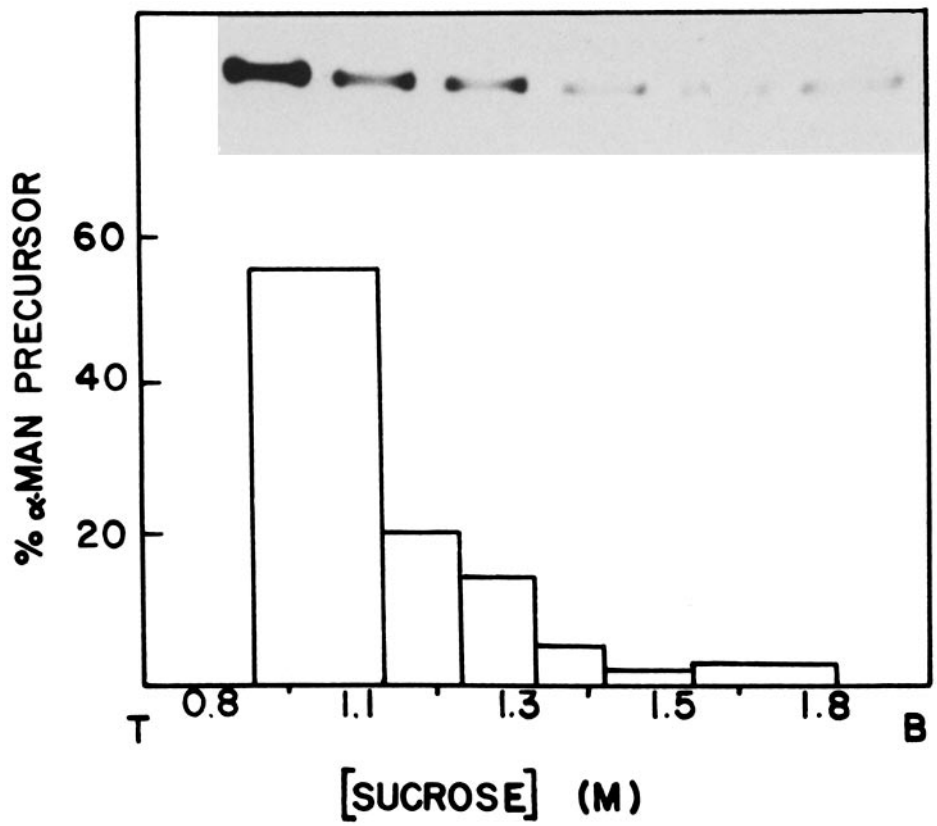


FIGURE 7 Accumulation of pulse-labeled α-mannosidase precursor in the low density membrane fraction in the presence of potassium cyanide. Axenically growing cells were pulse-labeled with [$^{35}$S]methionine for 10 min and then incubated in unlabeled medium containing 5 mM potassium cyanide for 1 h. The cells were processed and the 100,000 *g* postnuclear membrane vesicles fractionated on a discontinuous sucrose gradient as described in Fig. 5 and in Materials and Methods. α-Mannosidase was immunoprecipitated from each gradient fraction and subjected to electrophoresis on a 7.5% SDS polyacrylamide gel, followed by fluorography, and quantitation of the 140-kD precursor bands (*inset*) by laser densitometry.

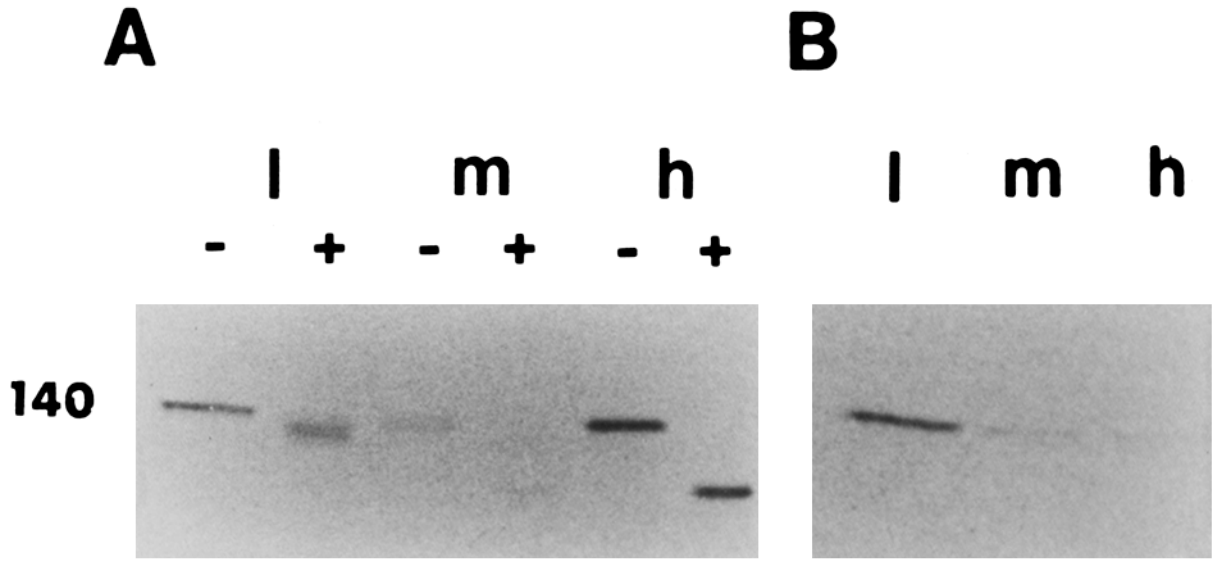


FIGURE 8 Sulfation of the precursor in the low density membrane fraction. In *A*, axenically growing cells were pulse-labeled with [$^{35}$S]methionine for 15 min and then incubated in unlabeled medium for 10 min. The cells were processed and the 100,000 *g* postnuclear supernatant membranes were fractionated on sucrose gradients as described in Fig. 5 and in Materials and Methods. Three fractions (low [*l*], medium [*m*], and high [*h*] density) were collected from the gradients corresponding to the top two, middle two, and bottom two fractions, respectively, of the gradients in Figs. 5–7. α-Mannosidase was immunoprecipitated from each fraction and ½ of the immunopurified sample treated with endo H as described in Fig. 3. In *B*, growing cells were pulse-labeled with $^{35}SO_4$ and fractionated as described above. All immunopurified samples were subjected to electrophoresis and fluorography as described in Materials and Methods.

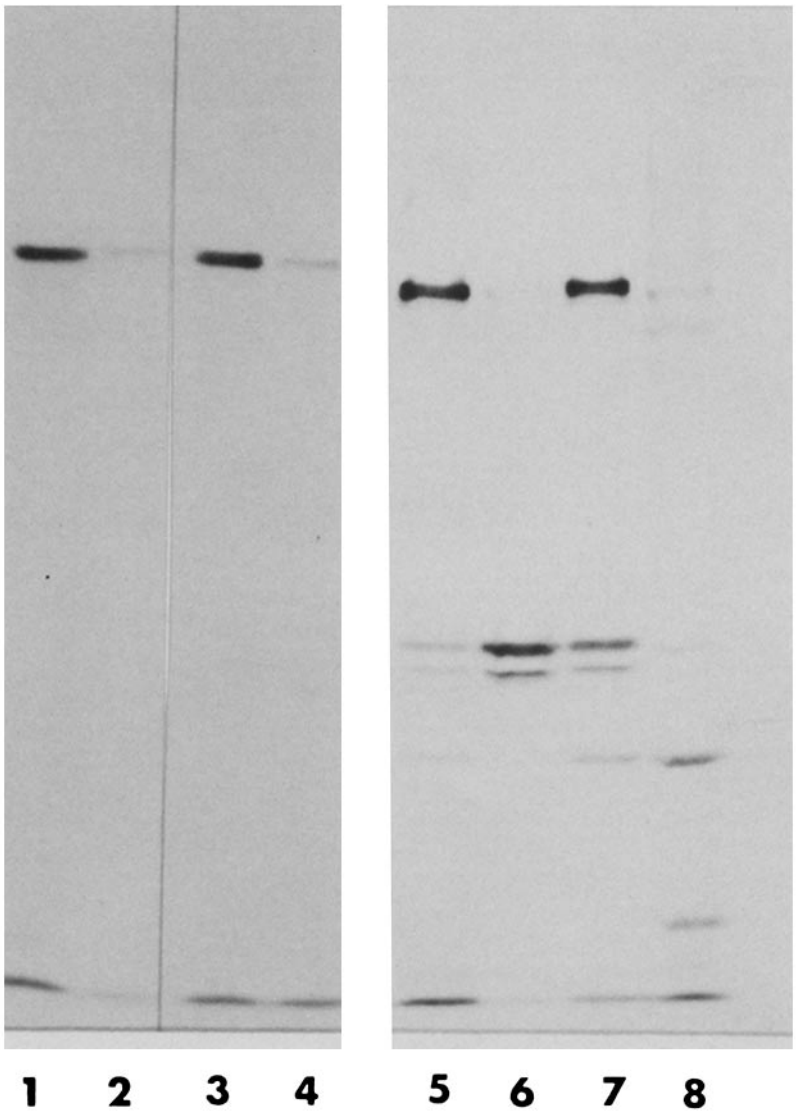


FIGURE 9 Association of the cellular α-mannosidase precursor with the vesicle membrane. Growing cells were labeled with [$^{35}$S]methionine for 10 min (lanes *1–4*) and 1 h (lanes *5–8*). Immediately after the labeling period, the cells were collected by centrifugation and washed once (half of the cells in isotonic buffer [TKM + 0.25 M sucrose] and the other half in water), followed by cell breakage by Dounce homogenization in the same solution. After removal of nuclei and unbroken cells, the homogenates were centrifuged at 100,000 *g* for 30 min. The supernatants were removed and the membrane pellets resuspended in the same buffer and recentrifuged at the same speed for 30 min. The supernatants were discarded and the washed pellets resuspended in the buffer used for immunoprecipitation. α-Mannosidase was immunoprecipitated from each pellet and original supernatant (soluble) fraction and subjected to electrophoresis on a 7.5% SDS polyacrylamide gel, followed by fluorography. Each pair of lanes represents the pellet and soluble fractions, respectively. Lanes *1*, *2*, *5*, and *6*, membranes prepared under hypotonic conditions; lanes *3*, *4*, *7*, and *8*, membranes prepared under isotonic conditions.

the fractionation, it seems unlikely for plasma membrane to be the site of precursor association described here. In support of our data, there is a large body of evidence showing a Golgi route for lysosomal enzymes as well as secretory and plasma membrane proteins subsequent to their synthesis on RER in mammalian cells (for reviews, see references 10, 11, 40).

The fact that newly processed (cleaved) mature enzyme appears to be compartmentalized in vesicles that cofractionate with mature lysosomes indicates that most if not all of the proteolytic cleavage of the precursor occurs in the Golgi complex immediately before transport, during transport, or immediately after arrival at the lysosome. We cannot, however, rule out the possibility that cleavage may occur in other organelles, such as coated vesicles or prelysosomes, that cofractionate with the Golgi, which would be intermediates in the transport pathway between the Golgi and mature lysosomes. Our results are consistent with those of Brown and Swank (3), who reported that the conversion of mouse macrophage β-glucuronidase and β-galactosidase precursors to mature forms is closely coupled with their lysosomal localization. In contrast, the relatively slow proteolytic maturation of cathepsin D in mouse spleen and β-glucuronidase in rat preputial gland occurs subsequent to lysosomal packaging (38). Also, the proteolytic processing of hexosaminidase (18) and cathepsin D (20) in fibroblasts appears to occur predominantly within the lysosomal compartment. In this connection, there also appears to be variability in the site(s) of processing for secretory proteins. Several polypeptide hormone precursors are cleaved to mature forms before their localization in secretory granules, while in other cases cleavage is completed within the granules (23, 26, 34, 44). The reasons why some proteins are processed before their final localization while others undergo cleavage afterwards remain unclear.

The finding that the α-mannosidase precursor is membrane associated while the newly cleaved mature subunits are soluble within the lumen suggests a critical role for precursor cleavage in localization that has not been previously described for a lysosomal enzyme. One targeting mechanism for mammalian enzymes involves their binding to membrane receptors via phosphomannosyl recognition markers (40), a pathway that appears to be unavailable in the slime mold due to the absence of receptors. Since mammalian enzymes reach the *cis* Golgi, a site of high receptor concentration (4), in precursor form, at least the initial targeting reactions must be performed with the precursor as substrate. Our results indicate that slime mold α-mannosidase is targeted to lysosomes through a different type of association of its precursor with Golgi membranes. This membrane association appears to be continuous

from the RER through transport to the Golgi and is ended intracellularly with the release of the mature subunits coincident with proteolytic cleavage. At present there are a number of possibilities for the nature of the interaction of the precursor with the membranes, including a membrane receptor that recognizes modifications, peptide sequences or conformations specific to the precursor, a lipid linked modification that could anchor the precursor in the membrane, or an uncleaved N-terminal signal sequence that remains as an anchor after translation.

The mechanism of membrane association must account for the secretion of a significant portion (up to 30%) of the precursor in soluble form within 30 min of synthesis. Our data suggest that the secreted and intracellular pools are sorted in the Golgi complex. The secreted precursor is packaged into a compartment that is distinct from lysosomes and this process is either the result of or attended by additional modification. Since the secreted precursor appears to be more heavily sulfated than that which is processed intracellularly, it is likely to have been exposed to sulfotransferases that apparently are not seen by the cellular form until immediately before or following cleavage. The larger apparent molecular weight of the secreted form reduces the likelihood of a proteolytic release from the membrane analogous to that of the mature enzyme. It should again be noted that the *Dictyostelium* lysosomal enzymes lack complex forms of N-glycosylation found in limited amounts on mammalian lysosomal enzymes (17), which precludes models involving these modifications. We cannot tell now whether the additional modifications are the cause or the result of packaging into this secretory pool. We also cannot rule out the possibility that the secreted and cellular forms may be translated from two functionally distinct mRNAs as in the case of some immunoglobulins (36), which may lead to their localization via interaction with different membrane components. It is clear, however, that all of the $\alpha$-mannosidase precursor is coded by a single structural gene. We have recently isolated various mutants, one of which diverts 100% of the precursor to rapid secretion, and another of which appears to be unable to transport the precursor out of the ER (unpublished results). Detailed analysis of these mutants may lend further insight into the mechanisms of targeting and secretion of this enzyme.

A targeting mechanism that is restricted to the precursor form explains the inability to find any type of receptor or binding protein for the mature enzyme, which has been used for previous studies. This mechanism may also explain the alternate processing pathway for lysosomal enzymes in mammalian cells. In addition, the presence of mannose-6-phosphate in this organism in the absence of a receptor may indicate that this modification has some function in lysosomal enzymes besides that related to targeting.

This research was supported by the College of Agricultural and Life Sciences, University of Wisconsin, Madison, and by the National Institutes of Health under grants GM 29156 and GM 31181. R. L. Dimond is the recipient of a Research Career Development Award from the National Institutes of Health.

*Received for publication 4 September 1984, and in revised form 11 January 1985.*

## REFERENCES

1. Amar-Costesec, A., H. Beaufay, M. Wibo, D. Thines-Sempoux, E. Feytmans, M. Robbi, and J. Berthet. 1974. Analytical study of microsomes and isolated subcellular membranes from rat liver. II. Preparation and composition of the microsomal fraction. *J. Cell Biol.* 61:201–212.
2. Borts, R. H., and R. L. Dimond. 1981. Identification and characterization of the $\alpha$-glucosidases of *Dictyostelium discoideum*. II. Developmental regulation and cellular localization. *Dev. Biol.* 87:185–192.
3. Brown, J. A., and R. T. Swank. 1983. Subcellular redistribution of newly synthesized macrophage lysosomal enzymes. Correlation between delivery to lysosomes and maturation. *J. Biol. Chem.* 258:15323–15328.
4. Brown, W. J., and M. G. Farquhar. 1984. The mannose-6-phosphate receptor for lysosomal enzymes is concentrated in cis Golgi cisternae. *Cell.* 36:295–307.
5. Burns, R. A., G. P. Livi, and R. L. Dimond. 1981. Regulation and secretion of early developmentally controlled enzymes during axenic growth in *Dictyostelium discoideum*. *Dev. Biol.* 84:407–416.
6. Carey, D. J., and C. B. Hirschberg. 1981. Topography of sialoglycoproteins and sialotransferases in mouse and rat liver Golgi. *J. Biol. Chem.* 256:989–993.
7. Dimond, R. L., R. A. Burns, and K. B. Jordan. 1981. Secretion of lysosomal enzymes in the cellular slime mold, *Dictyostelium discoideum*. *J. Biol. Chem.* 256:6565–6572.
8. Elting, J. J., W. W. Chen, and W. J. Lennarz. 1980. Characterization of a glucosidase activity involved in an initial step in the processing of oligosaccharide chains. *J. Biol. Chem.* 255:2325–2331.
9. Erickson, A. H., and G. Blobel. 1979. Early events in the biosynthesis of the lysosomal enzyme cathepsin D. *J. Biol. Chem.* 254:11771–11774.
10. Farquhar, M. G. 1983. Multiple pathways of exocytosis, endocytosis, and membrane recycling: validation of a Golgi route. *Fed. Proc.* 42:2407–2413.
11. Farquhar, M. G., and G. E. Palade. 1981. The Golgi apparatus (complex)—(1954–1981)—from artifact to center stage. *J. Cell Biol.* 91:77s–103s.
12. Fischer, H. D., A. Gonzalez-Noriega, and W. S. Sly. 1980. $\beta$-Glucuronidase binding to human fibroblast membrane receptors. *J. Biol. Chem.* 255:5069–5074.
13. Fischer, H. D., A. Gonzalez-Noreiga, W. S. Sly, and D. J. Morre. 1980. Phosphomannosyl-enzyme receptors in rat liver: subcellular distribution and role in intracellular transport of lysosomal enzymes. *J. Biol. Chem.* 255:9608–9615.
14. Fischer, H. D., M. Natowicz, W. S. Sly, and R. K. Bretthauer. 1980. Fibroblast receptor for lysosomal enzymes mediates pinocytosis of multivalent phosphomannan fragment. *J. Cell Biol.* 84:77–86.
15. Free, S. J., and W. F., Loomis, Jr. 1974. Isolation of mutations in *Dictyostelium discoideum* affecting $\alpha$-mannosidase. *Biochimie.* 56:1525–1528.
16. Freeze, H. H., A. L. Miller, and A. Kaplan. 1980. Acid hydrolases from *Dictyostelium discoideum* contain phosphomannosyl recognition markers. *J. Biol. Chem.* 255:11081–11084.
17. Freeze, H. H., R. Yeh, A. L. Miller, and S. Kornfeld. 1983. Structural analysis of the oligosaccharides from three lysosomal enzymes of *Dictyostelium discoideum*: evidence for an unusual acid-stable phosphodiester. *J. Biol. Chem.* 258:14874–14879.
18. Frisch, A., and E. F. Neufeld. 1981. Limited proteolysis of the $\beta$-hexosaminidase precursor in a cell free system. *J. Biol. Chem.* 256:8242–8246.
19. Gabel, C. A., D. E. Goldberg, and S. Kornfeld. 1983. Identification and characterization of cells deficient in the mannose 6-phosphate-receptor: evidence for an alternate pathway of lysosomal enzyme targeting. *Proc. Natl. Acad. Sci. USA.* 80:775–779.
20. Gieselmann, V., R. Pohlmann, A. Hasilik, and K. von Figura. 1983. Biosynthesis and transport of cathepsin D in culture human fibroblasts. *J. Cell Biol.* 97:1–5.
21. Green, E. D., J. Gruenbaum, M. Bielinska, J. U. Baenziger, and I. Boime. 1983. Sulfation of lutropin oligosaccharides with a cell-free system. *Proc. Natl. Acad. Sci. USA.* 81:5320–5324.
22. Grinna, L. S., and P. W. Robbins. 1979. Glycoprotein biosynthesis: rat liver microsomal glucosidases which process oligosaccharides. *J. Biol. Chem.* 254:8814–8818.
23. Gumbiner, B., and R. B. Kelly. 1981. Secretory granules of an anterior pituitary cell line, AtT-20, contain only mature forms of corticotropin and $\beta$-lipotropin. *Proc. Natl. Acad. Sci. USA.* 78:318–322.
24. Hasilik, A., and E. F. Neufeld. 1980. Biosynthesis of lysosomal enzymes in fibroblasts: synthesis as precursors of higher molecular weight. *J. Biol. Chem.* 255:4937–4945.
25. Ikeda, T. 1981. Subcellular distributions of UDP-galactose: polysaccharide transferase and UDP-glucose pyrophosphorylase involved in biosynthesis of prespore-specific acid mucopolysaccharide in *Dictyostelium discoideum*. *Biochim. Biophys. Acta.* 675:69–76.
26. Julius, D., R. Schekman, and J. Thorner. 1984. Glycosylation and processing of prepro-$\alpha$-factor through the yeast secretory pathway. *Cell.* 36:309–318.
27. Kaplan, A., D. T. Achord, and W. S. Sly. 1977. Phosphomannosyl components of a lysosomal enzyme are recognized by pinocytosis receptors on human fibroblasts. *Proc. Natl. Acad. Sci. USA.* 74:2026–2030.
28. Laemmli, U. K. 1970. Cleavage of structural proteins during the assembly of the head of bacteriophage T4. *Nature (Lond.).* 227:680–685.
29. Loomis, W. F., Jr. 1970. Developmental regulation of $\alpha$-mannosidase in *Dictyostelium discoideum*. *J. Bacteriol.* 103:375–381.
30. Mierendorf, R. C., Jr., J. A. Cardelli, G. P. Livi, and R. L. Dimond. 1983. Synthesis of related forms of the lysosomal enzyme $\alpha$-mannosidase in *Dictyostelium discoideum*. *J. Biol. Chem.* 258:5878–5884.
31. Mierendorf, R. C., Jr., and R. L. Dimond. 1983. Functional heterogeneity of monoclonal antibodies obtained using different screening assays. *Anal. Biochem.* 135:221–229.
32. Pannell, R., L. Wood, and A. Kaplan. 1982. Processing and secretion of $\alpha$-mannosidase forms by *Dictyostelium discoideum*. *J. Biol. Chem.* 257:9861–9865.
33. O'Farrell, P. H. 1975. High resolution two-dimensional electrophoresis of proteins. *J. Biol. Chem.* 250:4007–4021.
34. Ravazzola, M., R. Benoit, N. Ling, R. Guillemin, and L. Orci. 1983. Immunocytochemical localization of prosomatostatin fragments in maturing and mature secretory granules of pancreatic and intestinal D cells. *Proc. Natl. Acad. Sci. USA.* 80:215–218.
35. Robbins, A. R., and R. Myerowitz. 1981. The mannose 6-phosphate receptor of Chinese hamster ovary cells: compartmentalization of acid hydrolases in mutants with altered receptors. *J. Biol. Chem.* 256:10623–10627.
36. Rogers, J., P. Early, C. Carter, K. Calame, M. Bond, L. Hood, and R. Wall. 1980. Two mRNAs with different 3′ ends encode membrane-bound and secreted forms of immunoglobulin $\mu$ chain. *Cell.* 20:303–312.
37. Rome, L. H., B. Weissman, and E. F. Neufeld. 1979. Direct demonstration of binding of a lysosomal enzyme, $\alpha$-L-iduronidase, to receptors on cultured fibroblasts. *Proc. Natl. Acad. Sci. USA.* 76:2331–2334.
38. Rosenfeld, M. G., G. Kreibich, D. Popov, K. Kato, and D. D. Sabatini. 1982. Biosynthesis of lysosomal hydrolases: their synthesis in bound polysomes and the role of co- and posttranslational processing in determining their subcellular distribution. *J. Cell Biol.* 93:135–143.
39. Rothman, J. E., and E. Fries. 1981. Transport of newly synthesized vesicular stomatitis viral glycoprotein to purified Golgi membranes. *J. Cell Biol.* 89:162–168.

40. Sabatini, D. D., G. Kreibich, T. Morimoto, and M. Adesnik. 1982. Mechanisms for the incorporation of proteins in membranes and organelles. *J. Cell Biol.* 92:1–22.
41. Sabatini, D. D., Y. Toshiro, and G. E. Palade. 1966. On the attachment of ribosomes to microsomal membranes. *J. Mol. Biol.* 19:503–524.
42. Sahagian, G. G., and E. F. Neufeld. 1983. Biosynthesis and turnover of the mannose 6-phosphate receptor in cultured Chinese hamster ovary cells. *J. Biol. Chem.* 258:7121–7128.
43. Skudlarek, M. D., and R. T. Swank. 1979. Biosynthesis of two lysosomal enzymes in macrophages: evidence for a precursor of β-galactosidase. *J. Biol. Chem.* 254:9939–9942.
44. Steiner, D. F. 1976. Peptide hormone precursors: biosynthesis, processing and significance. *In* Peptide Hormones. J. A. Parsons, editor. University Park Press, Baltimore, MD.
45. Wood, L., R. N. Pannell, and A. Kaplan. 1983. Linked pools of processed α-mannosidase in *Dictyostelium discoideum*. *J. Biol. Chem.* 258:9426–9430.